

1 **Limitations of Persistent Scatterer Interferometry to measure small seasonal ground movements**
2 **in an urban environment**

3 J M Scoular^{1*}, J Croft¹, R C Ghail², P J Mason³, J A Lawrence¹, I Stoianov¹

4 ¹Department of Civil and Environmental Engineering, Imperial College London, London, SW7 2AZ, UK

5 ²Department of Earth Sciences, Royal Holloway, University of London, TW20 0EX

6 ³Department of Earth Science and Engineering, Imperial College London, London, SW7 2AZ, UK

7 *Corresponding author (e-mail: Jennifer.scoular13@imperial.ac.uk)

8
9 **Abstract:** London Clay, which underlies the majority of Greater London, has a high shrink-swell
10 potential that can result in damage to foundations and surface infrastructure due to seasonal
11 expansion and contraction of the clay. Currently, surface movement as a result of shrink-swell is not
12 monitored in London, meaning that the magnitude and cyclicity of these movements is poorly
13 understood. Persistent Scatterer Interferometric Synthetic Aperture Radar (PSI) data provide high-
14 precision line-of-sight displacement measurements at a high point density across urban areas,
15 offering the possibility of routine shrink-swell monitoring across whole cities. To test this, PSI data
16 derived from TerraSAR-X (TSX) observations for the period from May 2011 to April 2017 were
17 analysed for shrink-swell patterns across three areas of London in Hammersmith, Muswell Hill and
18 Islington. A consistent cyclicity and amplitude was detected at all sites and the number of cycles is
19 comparable with those identified in rainfall data. The amplitude of these cycles is smaller than
20 anticipated, most probably because of the resisting effect of roads and pavements. The Cranfield
21 University Leakage Assessment from Corrosivity and Shrinkage (LEACS) database was used to
22 subdivide the PSI data and the average velocity and amplitude of each class statistically tested for
23 significant differences between classes. The results show that it is not possible to statistically isolate
24 possible soil shrink-swell movement in TSX PSI data in London.

26 Shrink-swell of clays is known to cause structural damage to buildings and infrastructure and is a
27 major cause of water main pipe bursts (Boyle et al. 2000). It poses the highest cost and subsequent
28 risk to infrastructure systems in the UK, with the potential to exceed the economic costs of flooding
29 if climate change predictions are accurate (Pritchard et al. 2013). The National House Building
30 Council (NHBC), report that approximately 80% of foundation related claims it receives are due to
31 clay soil volume change (Driscoll & Crilly 2000). The UK climate projections UKCP09 predict hotter
32 drier summers in southern England, with summer rainfall decreasing by 12% and wetter winters,
33 with an overall yearly increase in rainfall, leading to more substantial shrink-swell cycles (Murphy et
34 al. 2009). All clays are subject to shrink and swell, but those with a higher proportion of expansive
35 clay minerals, such as smectite, experience much higher ratios of shrink-swell (Jones & Terrington
36 2011). In addition, tree cover, soil exposure, urbanisation and surface drainage factors, weather, and
37 atmosphere all influence the magnitude of wetting-drying cycles and hence the degree of shrink and
38 swell (Boyle et al. 2000). Clay-rich soils in the UK are most common in the south-east of England
39 (Harrison et al. 2009). London clay is particularly susceptible to shrink-swell and has long been the
40 cause of significant damage to foundations and infrastructure (Jones & Terrington 2011).

41 Despite its importance, there is a surprising lack of shrink-swell data for London Clay. Standard
42 methods for investigating such properties, such as BS 1377, 1990: Part 2, tests 6.3 & 6.4, Shrinkage
43 Limit and 6.5, Linear Shrinkage and Part 5, test 4, Swelling Pressure (British Standards Institution
44 1990), rarely form part of a routine site investigation in the UK (Jones & Terrington 2011).

45

46 The Volume Change Potential (VCP) of a soil is the relative change in volume to be expected with soil
47 moisture content flux, and is reflected in subsequent shrinkage and swelling of the ground (Jones &
48 Terrington 2011). Prior to Jones & Terrington (2011) there had been few studies on the VCP of
49 London Clay, except chapters covering the Plasticity Index (PI) in Burnett & Fookes (1974), Forster
50 (1997), Hight et al. (2003), Driscoll & Crilly (2000) and Pantelidou & Simpson (2007). Typical values of

51 PI for the London Clay are 46% to 63%, which equates to a High/Very High VCP (Driscoll & Crilly
52 2000).

53

54 Surface movement caused by shrink-swell in London Clay is also poorly quantified; in situ
55 measurements typically being restricted to infrastructure assets or areas in the vicinity of ongoing
56 construction and recorded for a limited time period only. Techniques such as levelling, total station
57 surveying, and GPS can provide accurate measurements of deformation, but can be costly if a high
58 density of measurements is required over a large area.

59

60 Precision GPS has been used to study ground movements in London but the spatial density of GPS
61 stations is low; only 26 in total, of which just 3 are relevant to clay shrink-swell (Ashkenazi et al.
62 1998). Boyle et al. (2000) used differential InSAR from ERS-1 and -2 to map surface movement in
63 London but the results were inconclusive and not validated. North et al. (2017) applied PSI to C-band
64 (5.6 cm) Sentinel-1 data to study the response of roads and railways to seasonal soil movement at 6
65 locations in the UK. Deformation was observed across all sites, with spatial and temporal patterns
66 caused by variations in regional water use and shrink-swell potential of the different soil types. Agar
67 (2018) identified swelling of Jurassic clays up to 10 mm/yr over an 8 month period in an area near Bath,
68 UK, using PSI applied to Sentinel-1 but the low PS point density (1063 PS/km²) limited interpretation
69 to the identification of regional trends (over a 50 x 40 km area), rather than local patterns.

70

71 High resolution Persistent Scatterer Interferometry (PSI) from X-band (3.1 cm) satellites can provide
72 a high density of high precision measurements over large areas. Although the shrink-swell signal is
73 anticipated to be smaller in urban compared to rural areas, the improved resolution of TerraSAR-X
74 (TSX) over Sentinel-1 or ERS should assist identification. This study investigates whether seasonal
75 cyclic movements in urbanised areas can be detected by TSX SAR data, processed by TRE Altamira

76 using SqueeSAR™. It uses statistical significance tests between detected ground movements and
77 different shrink-swell classes.

78

79 **Materials and Methods**

80 PSI data were obtained from TSX SAR data, processed by TRE Altamira using SqueeSAR™ (Ferretti et
81 al. 2011). TSX has a repeat period of 11 days and data for London were acquired in StripMap mode in
82 descending geometry at a spatial resolution of 3 m by 3 m (range and azimuth). Displacement along
83 the line of sight (LOS, incidence angle 37°) can be measured to better than 1 mm on PS characterised
84 by very consistent radar returns (Ferretti et al. 2001), with a standard deviation of 0.1 mm/yr on
85 range displacement rates. Apart from the consistency of the radar targets, the accuracy of the
86 measurements depends on the distance from the reference point and the quality of the filtering of
87 the atmospheric components in the interferograms (Colesanti et al. 2003; Ferretti et al. 2007a;
88 Ferretti et al. 2007b).

89

90 The data used in this study covers the time period from 1st May 2011 to 28th April 2017 (a total of
91 150 images, Figure 1) and have a minimum coherence of 0.8. Coherence is a measure of the phase
92 noise affecting the radar targets and ranges from 0, where the interferometric phase is just noise, to
93 1, where there is an absence of phase noise (Ferretti et al. 2007b). By selecting points exhibiting a
94 coherence value greater than 0.8, the standard deviation of the noise affecting each measurement is
95 expected to be better than 0.7 mm (Colesanti et al. 2003). Atmospheric filtering techniques in multi-
96 temporal InSAR analyses can mitigate the impact of these phase noise components on range
97 displacement data. However, some atmospheric leakage should always be considered. Atmospheric
98 disturbances are spatially correlated and cannot be reduced by spatial averaging. The decorrelation
99 distance of atmospheric components affecting SAR interferograms is about 4 km (Ferretti 2014).

100 Such errors can be reduced only by means of filtering procedures based on the statistical

101 characterisation of both the atmospheric disturbance and the signal of interest (Ferretti et al. 2001;

102 Ferretti et al. 2011). It should be noted that the atmospheric filtering procedure applied to the data-
103 set used in this work was not based on any pre-selected cyclic model for displacement of the radar
104 targets, to avoid creating a bias in the results. This TSX dataset has been validated with levelling data
105 (Bischoff 2019).

106

107 GIS vector point files, containing Persistent Scatterer (PS) velocity data, were supplied for three
108 areas in London (Hammersmith, Muswell and Islington); chosen to provide a good representative
109 sample of clays with different shrink-swell properties and differing long term ground movement
110 trends (Figure 2). The point density for each area was 3840 PS/km², 1930 PS/km² and 3830 PS/km²
111 for Hammersmith, Muswell and Islington respectively.

112

113 The National Soil Resources Institute (NSRI) holds the soil data for England and Wales in the Land
114 Information System (LandIS) database. Using topographic, climatic and LandIS soil data, Cranfield
115 University developed the Leakage Assessment from Corrosivity and Shrinkage (LEACS) database,
116 aimed specifically at the water industry, with soil shrink-swell recorded as just one of its parameters
117 (Dufour et al., 1998; Jarvis, 1999) in a GIS point vector file (Figure 2). Shrink-swell potential is
118 categorised from Very Low (1) to Very High (5), based on the predicted volumetric shrinkage that
119 occurs at soil suctions between 5 and 1500 kPa, as a percentage of the volume at 5 kPa (Hall et al.
120 1977; Jones & Hollis 2014). The thickness of superficial sequences, depth to rockhead and thickness
121 of London Clay were determined from borehole records from the British Geological Survey (BGS) and
122 Superficial Deposit Thickness data (British Geological Survey 2010), which was input into GIS with the
123 TSX data.

124

125 As the ground surface, rather than infrastructure, was the focus for this study, only PS points on
126 roads were used for analysis. PS points on buildings were discarded since they may be affected by
127 thermal dilation, may not be representative of surface motion depending on foundation depth and

128 because there is uncertainty as to where on the building the PS point is located. The location of
129 roads has been identified from the OS VectorMap District (Ordnance Survey 2018), which is a vector
130 line map of roads, input into GIS. The width of roads has been determined from the World
131 Topographic Map (1:1000) (Esri 2018) and the road lines of the OS VectorMap enlarged to that
132 width. The PS points were input into GIS and the overlapping road points were selected using the
133 *Intersect* function with the enlarged OS VectorMap. The number of road points in each area was
134 approximately 7,500 for Hammersmith, 1,500 for Muswell Hill and 30,000 for Islington, which
135 reduces the point density in each area to 1520 PS/km², 500 PS/km² and 1440 PS/km² respectively.

136

137 The PSI data were detrended, which removes the average secular ground movement of each area
138 over the entire time period. This was done because the focus is for short period ground movements,
139 not long-term trends. Processes that effect long term patterns of deformation in south-east England
140 include glacio-isostatic adjustment, tectonic processes, changes in groundwater levels, natural
141 compaction of alluvial deposits and anthropogenic loading or excavation (Bingley et al. 1999; Aldiss
142 et al. 2014; Mason et al. 2015). The number of cycles per year and the average amplitude of these
143 cycles, for each area, was calculated using the *Rainflow* function in Matlab (ASTM International 1985
144 (2011)), which detects a change in gradient from positive to negative or vice versa, with the number
145 of cycles per year being half the number of gradient changes. The Lomb Scargle method (Lomb 1976)
146 was used to test for periodicity to identify seasonal patterns in the PS data. This method is similar to
147 a Fast Fourier Transform (FFT) but it does not require equally spaced samples and allows for missing
148 data points.

149

150 Hourly rainfall data were acquired for the Heathrow weather station (station ID: 708) for the period
151 2011 to 2017, from the Met Office Integrated Data Archive System (MIDAS) through the Centre for
152 Environmental Data Analysis (CEDA) Web Processing Service (WPS) (Met Office 2006). The hourly
153 totals have been combined to obtain a daily rainfall total for the period midnight to midnight. As the

154 displacement measurements are every 11 days, a moving average of rainfall with a window size of
155 10 days is used and the value of this average, on the date where there is a displacement
156 measurement, are used in the comparison. Daily temperature data for Heathrow were also acquired
157 from MIDAS. A maximum and minimum temperature is recorded for the period with the end time
158 09:00 (overnight) and 21:00 (daytime). The maximum temperature during the daytime (9am to 9pm)
159 was used for temperature analysis in this study. To compare rainfall and displacement, the datasets
160 were first standardised by subtracting the mean and dividing by the standard deviation. Cross
161 correlation was performed using the *correlate*, function in the *Signal* module of *SciPy*, in Python 3.6
162 (Jones et al. 2001). Periodicity in rainfall and temperature was tested using the Lomb Scargle method
163 (Lomb 1976).

164

165 To test for a statistical significance in the average velocity and amplitude of PS points in different
166 shrink-swell units, points were group-selected according to their LEACS shrink-swell potential and a
167 one-way analysis of variance (ANOVA) test was applied to compare the averages across different
168 mapping units. The ANOVA test determines whether there are statistically significant differences
169 between two or more groups (the null hypothesis is that there is no difference in the means). If the p
170 value of the ANOVA test is significant, a post-hoc Tukey test is applied to determine exactly which
171 units are significantly different. A confidence level of 0.05 is used in all statistical tests.

172

173 **Results**

174 ***Average Ground Movements, Cyclicity and Periodicity***

175 Each area has a different long-term trend (Figure 3). Hammersmith has subsided by *ca* 4 mm over
176 the 6 years, whereas Muswell has uplifted by *ca* 2 mm and Islington has remained stable. The
177 detrended signals for each area show similar patterns of peaks and troughs, and magnitude of
178 movement that might imply common environmental controls on cyclicity, such as rainfall or
179 temperature.

180

181 The number of cycles per year is consistent between the sites, with an average of 8.5 per year over
182 the 5-year period (Table 1). The average amplitude between sites is also consistent at between 0.34
183 and 0.37 mm. An annual periodicity is evident only in Hammersmith, with a peak at 365 days (Figure
184 4), but all sites show a periodicity approximately at the two-year mark (600 to 700 days). There are
185 no other dominant signals at periods shorter than 365 days in any of the areas.

186

187 ***Comparison of detrended displacement with rainfall and temperature***

188 The Lomb-Scargle periodogram of daily rainfall reveal a weak annual periodicity but a strong spike in
189 power spectral density at approximately two years (Figure 5). The periodogram of daily temperature
190 reveal a clear annual periodicity (Figure 5).

191

192 The standardised displacement and 10-day rainfall moving average (Figure 6) suggest displacement
193 may be weakly correlated with rainfall but with a lag of just over a month. When this correlation is
194 statistically tested using Spearman's Rank, the correlation coefficients are very small: 0.089, 0.067
195 and 0.071 for Hammersmith, Muswell and Islington respectively. Cross correlation analysis between
196 rainfall and displacement reveal no significant correlation at any lag time (Figure 7).

197

198 The average number of rainfall cycles from the Heathrow dataset is 8 per year, which is comparable
199 to the number identified in the ground movement data (Table 1).

200

201 ***Comparison of Shrink-swell mapping units***

202 *Velocity*

203 Table 2 shows the areas with a statistically significant ($p < 0.05$) difference between shrink-swell
204 potential classes. If PS velocity correlated strongly with shrink swell, each class should be significant.

205

206 In Hammersmith there is a statistically significant difference between the Very Low and Low classes
207 ($p = 0.022$), which equates to 0.02 mm/yr. In Muswell, the differences in velocity are greater, for
208 example, the average velocity for both the Moderate and the Very High shrink-swell potential are
209 significantly larger than the Very Low shrink-swell potential ($p < 0.001$ for both). The difference in
210 velocity is approximately 0.14 mm/yr but the difference between Moderate and Very High at
211 Muswell is not significant.

212

213 In Islington, the difference in average velocity for the shrink-swell potential between the High and
214 Very Low classes is significant ($p < 0.001$), but the Low and Very Low classes are not significant.

215

216 *Amplitude*

217 The average amplitude for the shrink-swell potential classes is not significant in all areas (Table 3).
218 Hammersmith has a significant difference between the Low and Very Low shrink potential classes (p
219 < 0.001). Conversely, in Islington none of the shrink-swell units (High, Low and Very Low) are
220 significantly different ($p > 0.05$). If shrink-swell had a noticeable effect on amplitude, a significant
221 difference would be expected between each unit.

222

223 Additionally, not all areas that had a statistically significant difference in velocity exhibited a
224 significant difference in amplitude, such as the Islington High and Very Low classes. It is important to
225 note that many of the significant differences equate to very small ground movements, e.g. the
226 difference between the statistically significant Very Low and Moderate shrink-swell classes in
227 Muswell is just 0.08 mm, which is below the resolution of the data and therefore questionable.

228

229 *Different areas of the same class*

230 The average amplitudes of different areas in the same shrink-swell class are also compared (Table 4).

231 The data show a significant difference between the Low and Very Low ($p < 0.001$ and $p = 0.006$,

232 respectively) in Hammersmith and Islington. This is unexpected as areas in the same shrink-swell
233 class should show ground movement of a similar magnitude, but comparisons could only be made
234 for four of the areas.

235

236 **Discussion**

237 Cyclic ground movements are successfully identified in PS data but the amplitude of these cycles is
238 smaller than anticipated. This could be due to a non-perfect filtering of atmospheric phase
239 components in the InSAR analysis, but we deem it partly due to the location of the points, in that all
240 lie on the road surface, so any clay movement is likely resisted by Made Ground beneath. In London,
241 Made Ground thickness varies from <1 m to >10 m (Howland 1991). Additionally, with a temporal
242 resolution on the measurements of just 11 days, short-term periodicity may not be detected.

243

244 The number of cycles per year in the PS data is consistent with the number of cycles in the rainfall
245 data which suggests a connection between the two variables. Visual inspection of rainfall moving
246 average and displacement reveals a weak relationship between the two variables, with displacement
247 appearing to lag approximately one month behind rainfall. Despite this, neither Spearman's Rank or
248 cross-correlation analysis identify a statistically significant relationship between them.

249

250 There are many factors affecting the potential connection between these variables. The rainfall
251 measurement, at Heathrow, is approximately 15 to 25 km away from the study areas, so some local
252 variation is likely. Surface water drainage patterns have not been considered and there are other
253 factors which may affect road surface movements, such as thermal expansion. Additionally, the
254 correlation is performed on a moving average of total rainfall and the detrended displacement is an
255 average across thousands of points over an area of between 3 and 20 km².

256

257 The reason that only Hammersmith demonstrates an annual periodicity remains unclear. Its
258 proximity to the River Thames may lead to a larger surface water flow or a stronger tidal influence
259 on groundwater that increases the shrink-swell of the clays, and this may be further amplified by
260 subsidence from groundwater abstraction (Figure 2). Of the three areas it also has the thickest
261 alluvium and river terrace deposits (as determined from boreholes records and the BGS *DigiMap*
262 *Superficial Deposits* (British Geological Survey 2010)), although it has only moderate thickness of
263 London Clay. Muswell has the thickest London Clay, at 42 m (BGS borehole TQ28NE9), with
264 Hammersmith 38 m (TQ27NW419, TQ27NW87 and TQ27NW233) and Islington 19 m (TQ38SW497,
265 TQ38SW4239 and TQ38SW4048) but all areas have an approximately two-year periodicity,
266 consistent with rainfall.

267

268 These results suggest that shrink-swell is not detectable with PSI over London, despite the greater
269 sensitivity and PS density in urban areas, compared to rural areas. Urban drainage and the road base
270 structure reduces the amplitude and therefore suppresses the signal of shrink-swell movements to
271 below detectable limits. Additionally, the areas of interest are relatively small, which can make it
272 difficult to separate the signal of interest from spurious atmospheric components and only one area
273 was categorised as having a high shrink-swell potential; thus AOI size may be a limiting factor in
274 successful identification. Furthermore, the cyclicity detected may not actually be caused by shrink-
275 swell at all. Alternative causes for that cyclicity are not fully clear, but a relationship between small-
276 scale cyclic ground movements and rainfall has been demonstrated.

277

278 **Conclusions**

279 This study identifies a cyclicity in detrended ground movement from PSI in London. There are on
280 average 8 cycles of movement per year with amplitudes between 0.34 and 0.38 mm. Although these
281 figures are close to the precision of the data set, the number of cycles is consistent with annual
282 rainfall cycles. Detrended ground movements and rainfall data also show a statistically significant

283 two-year periodicity. The effect of shrink-swell classification on velocity and amplitude of ground
284 movements is inconclusive, some areas exhibit a statistically significant difference between classes,
285 but others do not. While some cyclical signal is apparent, monitoring shrink-swell in London using
286 TSX PSI data from road surfaces is not yet practicable but may be achievable using future
287 constellations of high-resolution SAR instruments with much shorter revisit times, and with
288 improved techniques for detecting complex, non-linear ground movements.

289

290 **References**

291 Agar, S. 2018. PSInSAR remote sensing observations into deformation behaviour at Salisbury Plain,
292 UK. *Chalk 2018 Conference*. ICE, Imperial College London, UK.

293

294 Aldiss, D., Burke, H., Chacksfield, B., Bingley, R., Teferle, N., Williams, S., Blackman, D., Burren, R., *et*
295 *al.* 2014. Geological interpretation of current subsidence and uplift in the London area, UK, as shown
296 by high precision satellite-based surveying. *Proceedings of the Geologists' Association*, **125**, 1-13,
297 <http://doi.org/10.1016/j.pgeola.2013.07.003>.

298

299 Ashkenazi, V., Bingley, R., Booth, S., Greenaway, R., Nursey, K., Bedlington, D., Ellison, R. &
300 Arthurton, R. 1998. Monitoring long term vertical land movements in the Thames Estuary and
301 Greater London. *FIG Commission*, 176-188.

302

303 ASTM International. 1985 (2011). Standard E1049. *Standard Practices for Cycle Counting in Fatigue*
304 *Analysis*, West Conshohocken PA.

305

306 Bingley, R.M., Ashkenazi, V., Penna, N.T., Booth, S.J., Ellison, R. & Morigi, A.N. 1999. *Monitoring*
307 *changes in Regional Ground Level, Using High Precision GPS*. Institute of Engineering Surveying and
308 Space Geodesy (IESSG), University of Nottingham and British Geological Survey (BGS).

309

310 Bischoff, C. 2019. *Monitoring ground movements and infrastructure in London, UK, using Permanent*
311 *Scatterer Interferometry*. Doctor of Philosophy (PhD), Imperial College London.

312

313 Boyle, J., Stow, R. & Wright, P. 2000. In-SAR Imaging of London Surface Movement for Structural
314 Damage Management and Water Resource Conservation. *Report for BNSC Link programme, project,*
315 **4, 7.**

316

317 British Geological Survey 2010. Superficial Thickness Advanced 1:50,000.
318 <https://digimap.edina.ac.uk/roam/download/geology>.

319

320 British Standards Institution. 1990. British Standard Methods of Test for Soils for Civil Engineering
321 Purposes. British Standards Institution.

322

323 Burnett, A.D. & Fookes, P.G. 1974. A regional engineering geological study of the London Clay in the
324 London and Hampshire Basins. *Quarterly Journal of Engineering Geology and Hydrogeology*, **7**, 257-
325 295.

326

327 Colesanti, C., Ferretti, A., Novali, F., Prati, C. & Rocca, F. 2003. SAR monitoring of progressive and
328 seasonal ground deformation using the permanent scatterers technique. *IEEE Transactions on*
329 *Geoscience and Remote Sensing*, **41**, 1685-1701.

330

331 Driscoll, R.M. & Crilly, M. 2000. *Subsidence damage to domestic buildings: lessons learned and*
332 *questions remaining*. CRC.

333

334 Esri 2018. World Topographic Map
335 <http://www.arcgis.com/home/item.html?id=30e5fe3149c34df1ba922e6f5bbf808f>.

336

337 Ferretti, A. 2014. *Satellite InSAR data: reservoir monitoring from space*. EAGE Publications.

338

339 Ferretti, A., Prati, C. & Rocca, F. 2001. Permanent scatterers in SAR interferometry. *IEEE Transactions*
340 *on Geoscience and Remote Sensing*, **39**, 8-20.

341

342 Ferretti, A., Monti-Guarnieri, A., Prati, C. & Rocca, F. 2007a. *InSAR Processing: A Practical Approach*.
343 The Netherlands: ESA Publications.

344

345 Ferretti, A., Monti-Guarnieri, A., Prati, C., Rocca, F. & Massonet, D. 2007b. *InSAR principles-guidelines*
346 *for SAR interferometry processing and interpretation*.

347

348 Ferretti, A., Fumagalli, A., Novali, F., Prati, C., Rocca, F. & Rucci, A. 2011. A new algorithm for
349 processing interferometric data-stacks: SqueeSAR. *IEEE Transactions on Geoscience and Remote*
350 *Sensing*, **49**, 3460-3470.

351

352 Forster, A. 1997. The Engineering Geology of the London Area 1: 50,000 Geological sheets 256, 257,
353 270, 271. *British Geological Survey Technical Report WN/97/27*.

354

355 Hall, D., Reeve, M., Thomasson, A. & Wright, V. 1977. *Water retention, porosity and density of field*
356 *soils*.

357

358 Harrison, M., Jones, L., Gibson, A., Cooper, A., Wildman, G. & Foster, C. 2009. GeoSure Version 5.
359 Methodology Review: Shrink Swell. *British Geological Survey Internal Report, IR/08/092*.

360

361 Hight, D., McMillan, F., Powell, J., Jardine, R. & Allenou, C. 2003. Some characteristics of London clay.
362 *Characterisation and engineering properties of natural soils*, **2**, 851-946.

363
364 Howland, A. 1991. London's Docklands: engineering geology. *Proceedings of the Institution of Civil*
365 *Engineers*, **90**, 1153-1178.

366
367 Jones, E., Oliphant, T. & Peterson, P. 2001. SciPy: Open source scientific tools for Python.
368 <http://www.scipy.org/>.

369
370 Jones, L. & Terrington, R. 2011. Modelling volume change potential in the London Clay. *Quarterly*
371 *Journal of Engineering Geology and Hydrogeology*, **44**, 109-122.

372
373 Jones, R.J.A. & Hollis, J.M. 2014. *Shrinkage and Clay-related subsidence risk*. Cranfield University
374

375
376 Lomb, N.R. 1976. Least-squares frequency analysis of unequally spaced data. *Astrophysics and space*
377 *science*, **39**, 447-462.

378
379 Mason, P.J., Ghail, R., Bischoff, C. & Skipper, J. 2015. Detecting and monitoring small-scale discrete
380 ground movements across London, using Persistent Scatterer InSAR (PSI).

381
382 Met Office. NCAS British Atmospheric Data Centre 2006. *MIDAS: UK Daily Rainfall Data*.
383 <http://catalogue.ceda.ac.uk/uuid/c732716511d3442f05cdeccbe99b8f90>,

384
385 Murphy, J.M., Sexton, D., Jenkins, G., Booth, B., Brown, C., Clark, R., Collins, M., Harris, G., *et al.*
386 2009. *UK climate projections science report: climate change projections*. Met Office Hadley Centre,
387 Exeter Report **1906360022**.

388
389 Natural Perils Directory Cranfield University Clay Soil Subsidence Hazard (Current Climate).
390 <http://www.landis.org.uk/services/npd.cfm>.

391
392 North, M., Farewell, T., Hallett, S. & Bertelle, A. 2017. Monitoring the Response of Roads and
393 Railways to Seasonal Soil Movement with Persistent Scatterers Interferometry over Six UK Sites.
394 *Remote Sensing*, **9**, 922.

395
396 Ordnance Survey. 2018. *OS VectorMap District*.

397
398 Pantelidou, H. & Simpson, B. 2007. Geotechnical variation of London Clay across central London.
399 *Géotechnique*, **57**, 101-112.

400
401 Pritchard, O.G., Hallett, S.H. & Farewell, T.S. 2013. *Soil movement in the UK—Impacts on critical*
402 *infrastructure*.

403

404 **Figure Captions**

405 **Fig. 1.** Distribution of the TerraSAR-X images over the time period May 2011 to April 2017. Notable
406 gap in data acquisition between January and July 2013.

407 **Fig. 2.** Study areas: (a) Hammersmith (b) Muswell and (c) Islington overlain on the LEACS shrink-swell
408 potential map (Natural Perils Directory Cranfield University) and the TerraSAR-X points overlain onto
409 the World Topographic Map (Esri 2018).

410 **Fig. 3.** Ground movement over the period May 2011 to April 2017 for Hammersmith (red), Muswell
411 (blue) and Islington (green) and the detrended average ground movement for each burst site.

412 **Fig. 4.** Lomb Scargle plot of detrended displacement suggesting an annual periodicity at
413 Hammersmith and a two-year periodicity at all sites.

414 **Fig. 5.** Lomb Scargle plot of daily rainfall and daily temperature at Heathrow weather station for the
415 period May 2011 to April 2017. Rainfall has a small peak at approximately one year, but a more
416 pronounced peak at approximately two years, similar to that of the detrended displacement.
417 Temperature has a strong annual periodicity (note the difference in strength of power spectral
418 density between the two graphs).

419 **Fig. 6.** Comparison of standardised rainfall with a moving average window of 10 and detrended
420 displacement for Hammersmith, Muswell and Islington.

421 **Fig. 7.** Result of cross-correlation analysis for Hammersmith, Muswell and Islington.

422 **Table 1** *Average number of cycles per year for each area (upper table) and average cycle amplitude*
423 *per year (mm) for each area (lower table)*

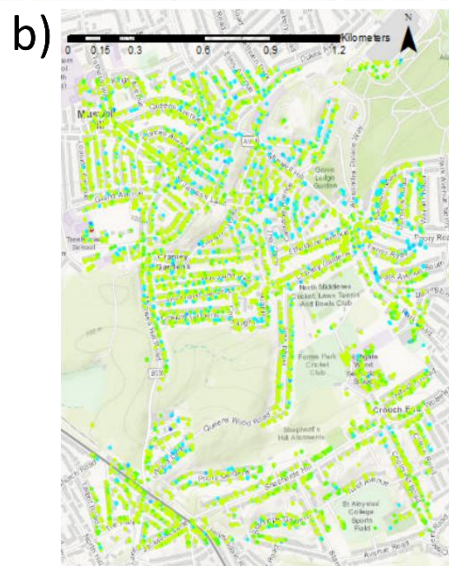
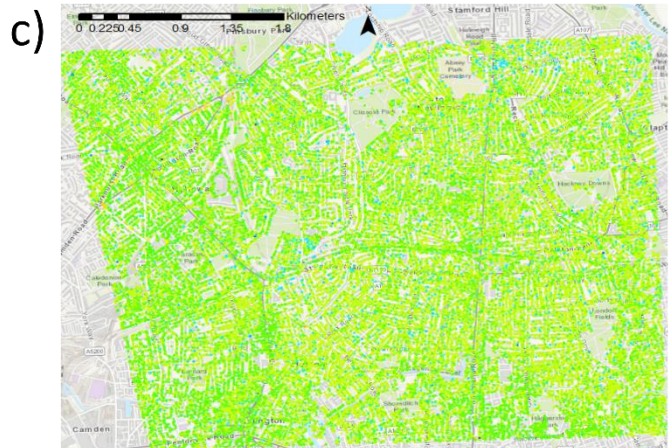
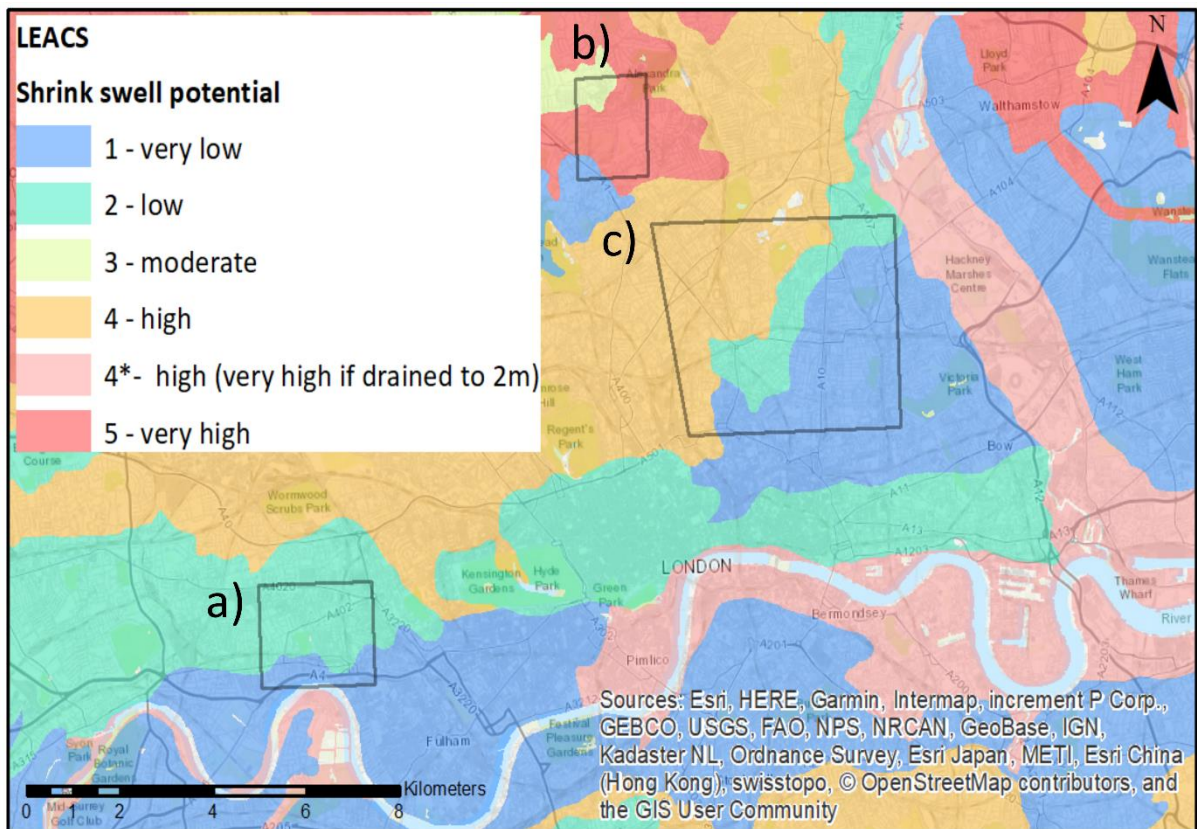
424 **Table 2** *Results of ANOVA and Tukey statistical tests comparing velocity between shrink-swell*
425 *potential classes. A result of $p < 0.05$ in the Tukey test implies the shrink-swell classes are significantly*
426 *different*

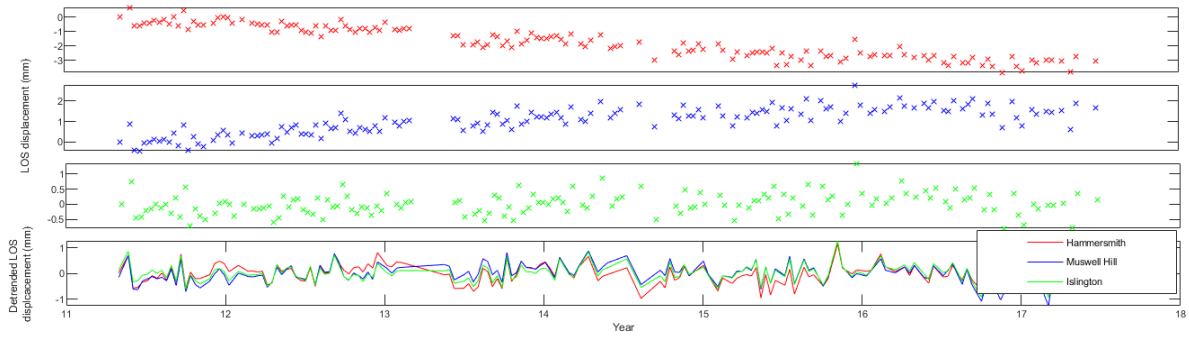
427 **Table 3** *Variations in statistical significance of average amplitude for shrink-swell classes*

428 **Table 4** *Significance of the difference in average amplitude for the same shrink-swell potential in*
429 *different areas*

430



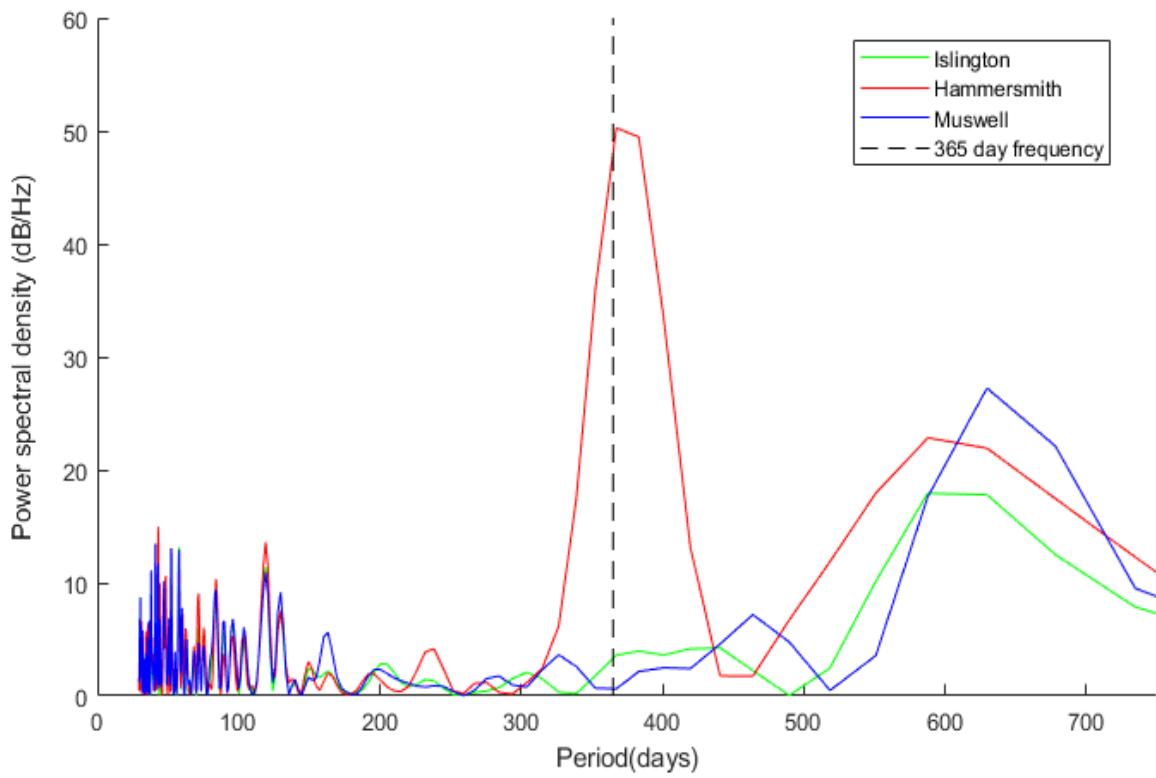




433

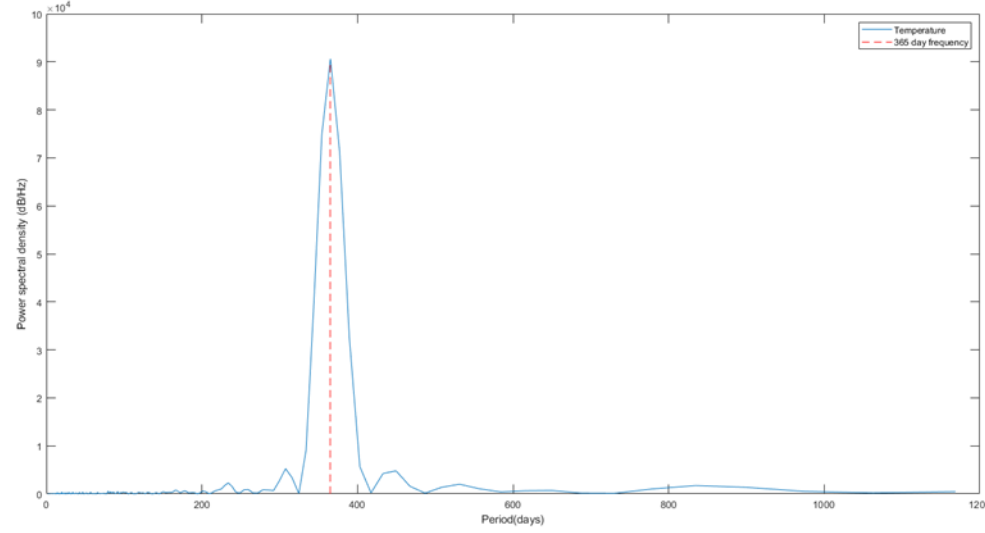
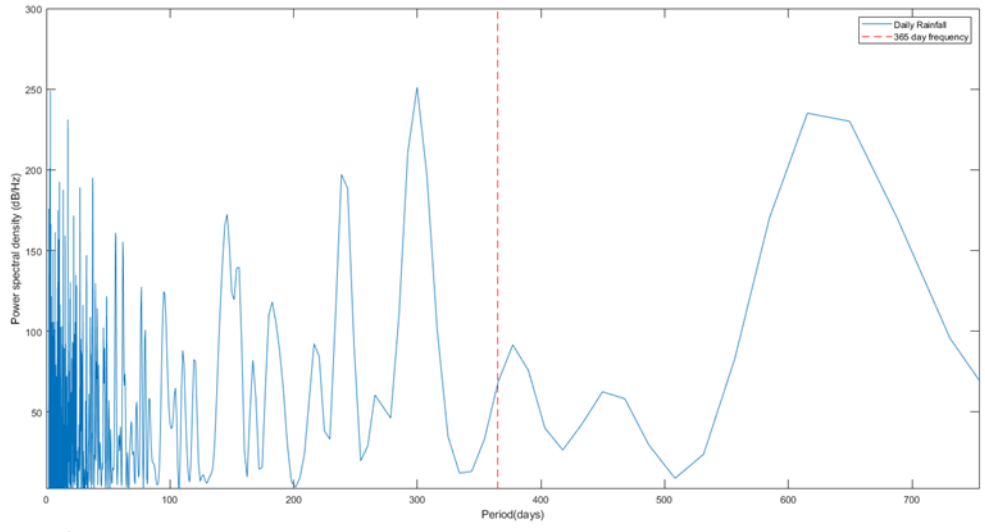
434

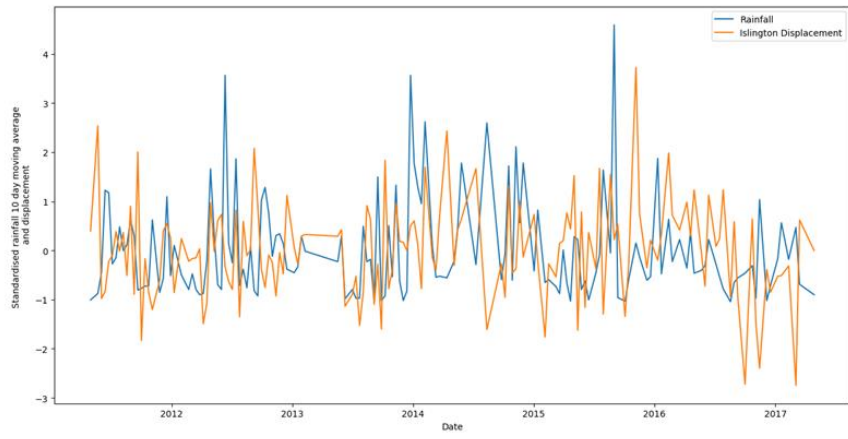
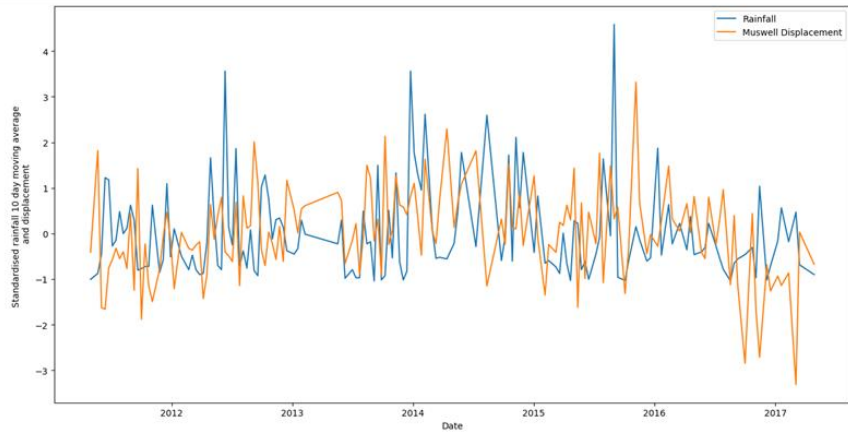
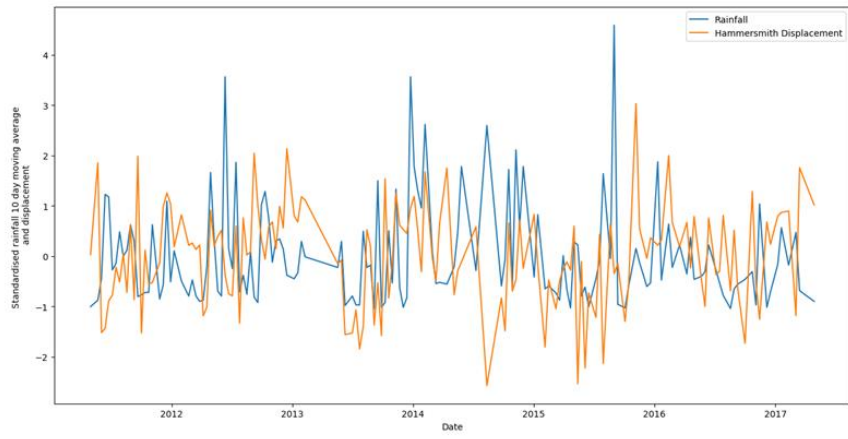
435

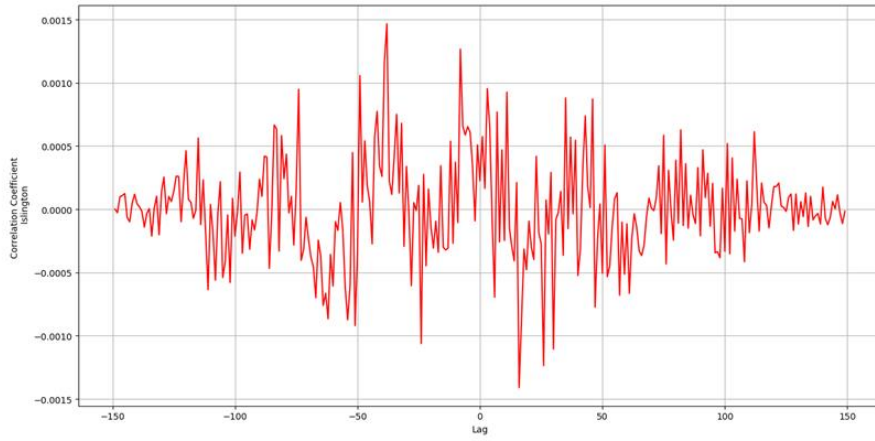
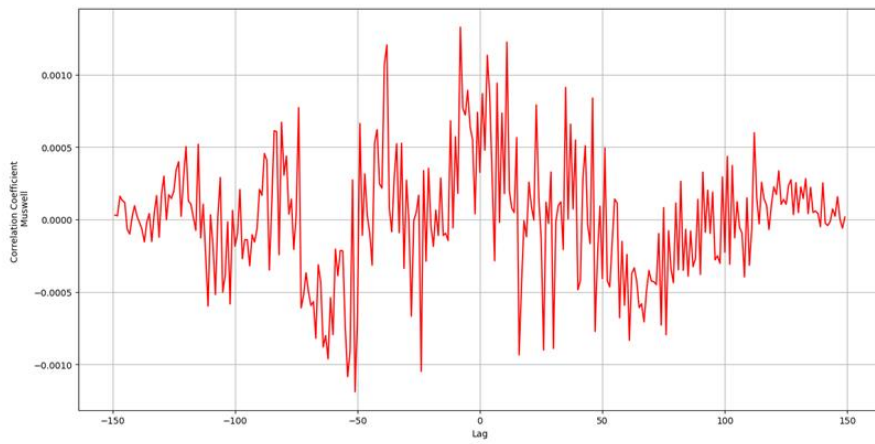
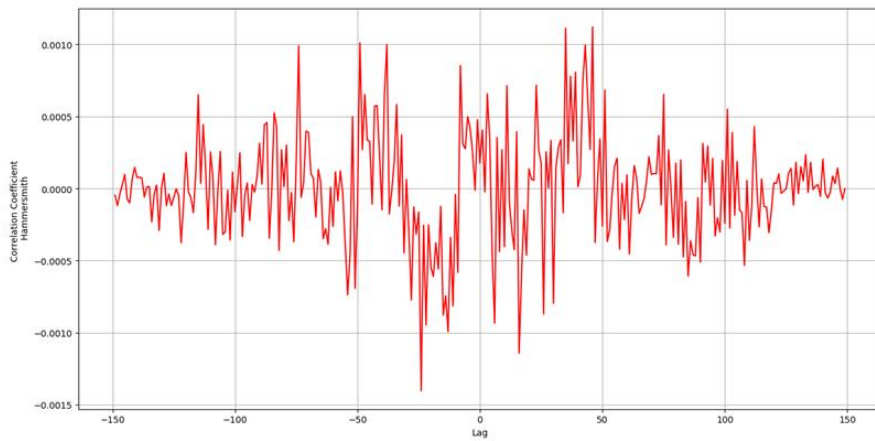


436

437







Year	Hammersmith	Muswell	Islington	Rainfall
2012	10.5	9.5	9.5	8.5
2013	8	7	8	8.5
2014	6.5	6.5	6.5	7
2015	10	11	10	8.5
2016	8	8	8	7
Average	8.6	8.4	8.4	7.9

Year	Hammersmith	Muswell	Islington
2012	0.31	0.29	0.27
2013	0.40	0.31	0.28
2014	0.38	0.38	0.35
2015	0.45	0.42	0.40
2016	0.32	0.43	0.39
Average	0.37	0.36	0.34

444

445

Variable 1	Variable 2	Mean 1	Mean 2	f-Anova	p-Anova	p-Tukey	Significant (Y/N)
Islington High	Islington Low	0.26	0.25	9.44	0.00	0.62	N
Islington High	Islington Very Low	0.26	0.24	9.44	0.00	0.00	Y
Islington Low	Islington Very Low	0.25	0.24	9.44	0.00	0.17	N
Muswell Very Low	Muswell Moderate	0.27	0.40	21.84	0.00	0.00	Y
Muswell Very Low	Muswell Very High	0.27	0.40	21.84	0.00	0.00	Y
Muswell Moderate	Muswell Very High	0.40	0.40	21.84	0.00	0.99	N
Hammersmith Low	Hammersmith Very Low	0.57	0.59	5.24	0.02	0.02	Y

Variable 1	Variable 2	Mean 1	Mean 2	f-Anova	p-Anova	p-Tukey	Significant (Y/N)
Muswell Very Low	Muswell Moderate	1.01	1.09	6.27	0.00	0.00	Y
Muswell Very Low	Muswell Very High	1.01	1.09	6.27	0.00	0.00	Y
Muswell Moderate	Muswell Very High	1.09	1.09	6.27	0.00	0.92	N
Islington High	Islington Low	1.03	1.03	0.47	0.62	-	N
Islington High	Islington Very Low	1.03	1.02	0.47	0.62	-	N
Islington Low	Islington Very Low	1.03	1.02	0.47	0.62	-	N
Hammersmith Low	Hammersmith Very Low	1.06	1.00	46.50	0.00	0.00	Y

447

Variable 1	Variable 2	Mean 1	Mean 2	f-Anova	p-Anova	p-Tukey	Significant (Y/N)
Hammersmith Low	Islington Low	1.06	1.02	45.97	0.00	0.00	Y
Muswell Very Low	Hammersmith Very Low	1.01	1.00	4.88	0.01	0.83	N
Muswell Very Low	Islington Very Low	1.01	1.02	4.88	0.01	0.83	N
Hammersmith Very Low	Islington Very Low	1.00	1.02	4.88	0.01	0.01	Y